Soft Tissues and Materials

JOURNAL OF
biomaterials
applications

Journal of Biomaterials Applications
2017, Vol. 32(5) 663–676

DOI: 10.1177/0885328217735933
journals.sagepub.com/home/jba
SAGE

Treatment of a burn animal model with functionalized tridimensional electrospun biomaterials

Daniela Steffens[1,2], Monica Beatriz Mathor[3], Paula Rigon da Luz Soster[4], Gustavo Vergani[5], Dayane Piffer Luco[6] and Patricia Pranke[1,2,6]

Abstract

Laminin-functionalized poly-D,L-lactic acid scaffolds were produced. Following this, mesenchymal stem cells and keratinocytes were seeded on biomaterials for the in vivo experiments, where the biomaterials with or without cells were implanted. The analysis is comprised of the visual aspect and mean size of the lesion plus the histology and gene expression. The results showed that the cells occupied all the structure of the scaffolds in all the groups. After nine days of in vivo experiments, the defect size did not show statistical difference among the groups, although the groups with the poly-D,L-lactic acid/Lam biomaterial had the lowest lesion size and presented the best visual aspect of the wound. Gene expression analysis showed considerable increase of tumor growth factor beta 1 expression, increased vascular endothelial growth factor and balance of the BAX/Bcl-2 ratio when compared to the lesion group. Histological analysis showed well-formed tissue in the groups where the biomaterials and biomaterials plus cells were used. In some animals, in which biomaterials and cells were used, the epidermis was formed throughout the length of the wound. In conclusion, these biomaterials were found to be capable of providing support for the growth of cells and stimulated the healing of the skin, which was improved by the use of cells.

Keywords

Stem cells, keratinocytes, skin substitute, electrospinning, tissue engineering

Introduction

The skin is the largest immunologically competent organ of the body. This tissue is basically formed of two layers: the epidermis and the dermis.

The epidermis is the outermost layer of the skin, it is compact and practically impermeable, forming the first physical barrier against external agents. It is composed of a keratinized squamous epithelium of ectodermal origin and consists of four distinct cell types, with the keratinocytes being considered the most important cells of the epidermis, accounting for 80% of the cells that make up this epithelium.[1–3]

The dermis, derived from the mesoderm, consists of a thick layer of connective tissue composed of large amounts of elastin and collagen, on which the epidermis rests. Within it are some elastic and reticular fibers, as well as many collagen fibers, where the blood and lymphatic vessels are present, besides numerous nerve endings. In the dermis are found endothelial cells, smooth muscle cells, mast cells, fibroblasts, and other cells of the immune system, as well as a large portion of the extracellular matrix. Fibroblasts are responsible for the synthesis of different macromolecules that make up the extracellular matrix and also have an intense activity during the cicatrization process.[2–5]

[1]Hematology and Stem Cell Laboratory, Faculty of Pharmacy, Universidade Federal do Rio Grande do Sul, RS, Brazil
[2]Post-graduate Program in Physiology, Universidade Federal do Rio Grande do Sul, Brazil
[3]Instituto de Pesquisas Energéticas e Nucleares – Institute of Nuclear Energy Research (IPEN), SP, Brazil
[4]Morphological Science Department, Universidade Federal do Rio Grande do Sul Porto Alegre, RS Brazil
[5]Faculdade de Medicina de Jundiaí, SP, Brazil
[6]Stem Cell Research Institute- Instituto de Pesquisa com Células-tronco. Porto Alegre, RS, Brazil

Corresponding author:
Daniela Steffens, Universidade Federal do Rio Grande do Sul, Ipiranga Av, 2752, lab 304G Porto Alegre, RS 90610000, Brazil.
Email: dani_ste@hotmail.com

These layers range in thickness, strength, and flexibility and thus provide the skin with a variety of functions.[6] Because the skin serves as a protective barrier to the outside world, any damage caused to it must be quickly and efficiently repaired.

Burn injuries occur annually to over 11 million people worldwide.

In cases of burns, high temperatures dilate the vessels and make the liquid contained in them leave, forming bubbles. These blisters can result in wounds, which are vulnerable to infection. The severity of burns is defined by the extent of damage to the victim.[7]

Furthermore, fibroblasts involved in tissue repair have the ability of producing large amounts of collagen but do not have the ability to organize these collagen fibers. The final result of the repair of the dermis is the disorganized deposition of collagen, which physically appears as tissue healing.

The time for wound closure is closely related to susceptibility to infections, duration of pain, hospital stay, and incidence of scarring.[8] Therefore, researchers around the world are working to improve currently available treatments through the development of new biomaterials for skin regeneration, bringing together the use of bioactive molecules and cell therapy,[9] with the aim of minimizing the occurrence of infections and scarring. These equivalent treatments can be categorized as epidermal, dermal, or composite, according to their structure and degree of functional similarity to normal skin. The commercial products commonly used are based on collagen, chitin, and fibrin.[3] Also, artificially manufactured products exist such as polylactic acid and polyglycolic acid, for example.[10]

In this work, poly-D,L-lactic acid (PDLLA) scaffolds produced by the electrospinning technique and also bound to laminin-332 protein (isoform $\alpha3\beta3\gamma2$) were developed.

The polymer used in this project was PDLLA, a biodegradable and biocompatible polyester with an amorphous structure.[11] It has previously been shown that PDLLA, pure or in a mixture, supports the growth of various cell types.[12–15]

To produce biomaterials by electrospinning, a polymeric solution is produced and submitted to the application of an electrical field, which promotes solvent evaporation and the formation of solid fibers that mimic the extracellular matrix structure. Following this, some structural modifications can be made, such as the adherence of a protein.

Laminin is the main protein found in the base membrane of the skin and it is fundamental for keratinocyte migration in the recovery of skin lesions.[16–18]

Several studies have demonstrated that this molecule is related not only to cell adhesion but also to the spreading, migration, and stimulation of cell growth rate, angiogenesis, healing, and neuronal growth.[19–21]

Moreover, as the cellular component of this future skin substitute, mesenchymal stem cells were chosen in order to fill the dermal part, as well as the keratinocytes to comprise the epidermal layer of the skin. It was therefore intended, through the construction of a biocompatible and biodegradable substitute and combined with the advantages of using laminin protein and cells, to develop a cutaneous substitute, which in future will be capable of regenerating cutaneous lesions of patients suffering from burns, among other uses.

Materials and methods

Production and functionalization of scaffolds

The construction of biodegradable biomaterials (matrices) for cell adhesion was conducted by the electrospinning method, as already demonstrated by Steffens et al.[22] The biomaterial was developed with two different diameters of fibers and, therefore, two polymer solutions were used: (1) PDLLA solution (molecular weight 75,000–120,000) in chloroform at a concentration of 30% (w/V) and (2) PDLLA solution (molecular weight 75,000–120,000) in dimethylformamide and tetrahydrofuran (1:1) at a concentration of 25% (w/V). For the electrospinning, the distance between the needle and the collector plate was approximately 20 cm for both solutions. For solution 1, a needle with an internal diameter of 0.7 mm was used, with a flow rate of 1 ml/h and electrical voltage of 20 kV. For the second solution, a needle with an internal diameter of 0.45 mm was used, with flow rate 1.25 ml/h and electrical voltage of 20 kV. The temperature to produce the scaffold was approximately 20°C. For the development of a bilayer scaffold, the fibers from solution 2 were formed on the upper surface of the matrix. After production of the matrices, two groups of scaffolds were developed: (1) PDLLA, as described above, without any change, and (2) PDLLA/Lam, a PDLLA matrix with subsequent hydrolysis of the fiber surface and binding of laminin protein.

To hydrolyze the surface of the biomaterials in the PDLLA/Lam group, a sodium hydroxide (NaOH) solution was used. With the aim of binding the laminin on the surface of the scaffolds in the PDLLA/Lam group, the hydrolysis and drying process were performed. A solution of ethyl (dimethylaminopropyl) carbodiimide (EDC) and N-hydroxysuccinimide (NHS) was then added to the scaffolds followed by a solution of laminin (Laminin 332, BioLamina®) 10 mg/ml and kept for 24 h.

Collection and cultivation of mesenchymal stem cells

For the present study, the MSCs were isolated from tissue pulp from deciduous teeth, as already described by Steffens et al.[22] The teeth were extracted from healthy children, enrolled on the Pediatric dentistry program of the Faculty of Dentistry at UFRGS, after informed written consent from the parents/guardians. After isolation, the adherent cells were cultivated in Dulbecco's Modified Eagle's Medium (DMEM) culture medium (D5523; Sigma Aldrich., St Louis, MO, USA) and supplemented with 10% bovine fetal serum (Gibco BRL, Grand Island, NY, USA) and 1% penicillin/streptomycin (Gibco BRL, Grand Island, NY, USA), at 37°C in a humid atmosphere of 5% CO_2. The culture medium was changed every three to four days. The passages were performed as required and the cells were tested for adipogenic, osteogenic, and chondrogenic differentiation as well as immunophenotyping profile (data not shown).

Keratinocyte cultivation

Cell suspensions were obtained from skin fragments devoid of breast subcutaneous tissue by serial enzymatic cell separation using a 0.05% trypsin/0.02% ethylenediaminetetraacetic acid (EDTA) solution (GIBCO-BRL Life Technologies, Rockville, MD, USA). The cells were plated at high density (5×10^4 cells/cm^2) in 25 cm^2 culture flasks in which the feeder-layer was previously cultivated.

The cell cultures were fed initially with a mixture of 60% DMEM (GIBCO-BRL Life Technologies), 30% Ham F12 (GIBCO-BRL Life Technologies), and 10% fetal bovine serum (HyClone™, GE Health Care Life Sciences), supplemented with 4 mM L-glutamine (GIBCO-BRL LifeTechnologies), 0.18 mM adenine (Sigma Chemical Co., St. Louis, MO, USA), 5 µg/ml insulin (Sigma), 0.4 µg/ml hydrocortisone (Sigma), 0.1 nM cholera toxin (Sigma), 2 nM tri-iodothyronine (Sigma), and 100 IU/ml penicillin/100 µg/ml streptomycin antibiotic solution (GIBCO-BRL Life Technologies). The culture bottles were stored in a 5% CO_2 incubator at 37°C. At the first medium change, the medium was further supplemented with 10 ng/ml epidermal growth factor (Sigma) and thereafter changed every 48 h.[23,24] These cells were cultivated in irradiated mouse embryonic fibroblast cells (CCL-92, ATCC®). The epidermal keratinocytes were used from the first to the third passage in the experiments.[22]

In vivo experiments

Incorporation of the cells in scaffolds for implantation in animal models. For in vivo experiments, the cell culture was maintained for seven days in an immersion culture system. The MSCs were cocultured with keratinocytes in the scaffolds. Initially, 100,000 MSCs were cultured on the bottom of the scaffolds together with coarser fibers. After 24 h, 100,000 keratinocytes were cultivated on the opposite side of the scaffold, i.e., the upper side (thinner fibers).

The use of human cells in biomaterials for subsequent application in mice was approved by the Ethics Committee at Universidade Federal do Rio Grande do Sul (No. CAAE 28783914.9.0000.5347). Animal experimentation was also approved by the Ethics Committee (No. 131/14) at Instituto de Pesquisas Energéticas e Nucleares.

Verification of the incorporation of cells in scaffolds. To verify the presence and morphology of the different cells in the scaffolds, the samples were examined by confocal microscopy. For this, three samples of PDLLA biomaterial and three samples of the PDLLA/Lam biomaterial were fixed with paraformaldehyde for 1 h at room temperature. Following, a solution of Triton in phosphate buffer solution (PBS) (PBS/Triton) (0.1%) was left in contact with the biomaterial for 30 min. Then phalloidin/rhodamine solution (200 µg/ml) in PBS/Triton solution, to cytoskeleton stain, was added to the wells containing the biomaterials for 40 min at room temperature and protected from light. After this period, the solution was removed and 4',6-diamidino-2-phenylindole (DAPI) was added for labeling the cell nuclei for a period of 1 min at room temperature, protected from light. Successive washes were performed and the biomaterials containing the labeled cells were kept refrigerated and away from light until the time of analysis.

Assessment of the capacity of mesenchymal stem cells and keratinocytes integrated in fiber scaffolds promote skin regeneration in an animal model of skin defect. Ten-week-old athymic mice were used, each weighing an average of 30 g. The mice were obtained from the animal house of the Instituto de Pesquisas Energéticas e Nucleares, in São Paulo.

In the presurgical period, the animals were kept for seven days in collective cages (maximum five animals per cage), having free access to water and feed, with day/night cycles (12 h/12 h) and temperature of 22 ± 2°C. For surgery, the animals were anesthetized with ketamine (1.16 g/10 ml) and xylazine (2.3 g/100 ml), combined and diluted in saline (1 ml ketamine + 1 ml xylazine to 8 ml saline). Anesthetic solution of 0.1 ml was used for each 10 mg of body weight intraperitoneally. In anesthesia conditions, a defect on the back of 1.0 × 1.0 cm was produced by excision with surgical scissors, removing all the skin to the muscle fascia, under surgical techniques. This skin defect simulates a third-degree burn.

The skin defect was immediately covered by the matrices, the size of which corresponding to the skin defect of 1.0 cm × 1.0 cm with approximately 200 μm in thickness. The scaffolds were set alongside adjacent normal skin by suture, a model described by Leonardi et al.[25] No further dressing was used on the graft since the scaffold itself already works as a barrier.[25–27] For the experiments, the animals were housed in the animal facility of IPEN in separate cages in the same conditions as previously mentioned.

In addition, the animals subcutaneously received saline containing the analgesic tramadol in a concentration of 10 mg/kg, immediately after implantation of the scaffold and every 12 h after the surgery for one day.

After a period of nine days, the animals were euthanized by anesthesia, using the same aforementioned dilutions of anesthetic, but in doses three times the usual anesthetic dose. All the animals were also subjected to the same pattern of euthanasia.

The following groups were studied, comprising six animals per group, except for group 1 and 6, where only four animals were used: Group 1—lesion control: animals with lesions where surgical gauze was used as a coating material; group 2—PDLLA/Lam: animals where the PDLLA/Lam scaffold was implanted without cells; group 3—PDLLA: animals where the PDLLA scaffold was implanted without cells; group 4—PDLLA/Lam + cells: animals where the PDLLA/Lam scaffold was implanted with MSCs and keratinocytes; group 5—PDLLA + cells: animals where the PDLLA scaffold was implanted with MSC cells and keratinocytes; and, group 6—healthy control: skin from the animals' dorsum, where the skin lesion was not performed. Used only for histology and gene expression tests.

Histological analyses. After euthanasia, a fragment containing the transition skin graft and the graft was removed from each animal. Part of the fragment was fixed in 10% buffered formalin (pH = 7.4) for 24 h. Consecutively, the biological sample was stained with hematoxylin–eosin for histological evaluation and kept for 24 h in 15% sucrose solution and then in 30% sucrose solution until frozen and cut in a cryostat solution. On the euthanasia day, a healthy skin fragment removed from the animals' backs from the other groups was also collected, corresponding to the healthy control group (Group 6). From each piece fixed in 10% formalin, two slides were prepared, each with five sections of 15 μm obtained in the cryostat.

Gene expression verification. The other half of the biological material was immediately placed in Trizol (Life Technologies) and frozen at −80°C until RNA extraction.

Total RNA for all the groups was extracted using Trizol® reagent (Invitrogen), after nine days of animal experimentation. Following this, all the RNA samples were quantified and their level of purity analyzed by spectrophotometry (NanoDrop). The cDNA was synthesized using reverse transcriptase M-MLV kit (Invitrogen), in accordance with the manufacturer's instructions.

After cDNA synthesis, the reaction efficiencies for all primers used were determined by optimizing the parameters so that the efficiency was between 95% and 105%. For determining glyceraldehyde 3-phosphate dehydrogenase (GAPDH) and type 1a pro-collagen (Col1a), 10 μl of SYBR green mix was used, 1 μl of primer mix, 0.5 μl ROX (internal control of the reaction), 1 μl of bovine serum albumin (BSA), 6.5 μl of water, and 1 μl of cDNA, producing a total of 20 ul reaction solution. For the other primers, such as stromal derived factor-1 (SDF-1), transforming growth factor-beta 1 (TGF-β1), BAX, and Bcl-2, 10 μl of SYBR green mix, 0.8 ul of primer mix, 0.5 μl of ROX, 1 μl of BSA, 6.7 μl of water, and 1 μl cDNA was used, totalling 20 μl per reaction. The analysis was performed with StepOnePlus equipment (Life Technologies). The reaction conditions were 50°C for 2 min, 95°C for 10 min, followed by 40 cycles of 95°C for 15 s and 60°C for 30 s. The melting curve was performed for all the reactions to ensure the homogeneity of the amplified product. The results were expressed as a relative expression of the gene groups, determined by the ΔΔCT method, using GAPDH as a housekeeping gene. The reactions were performed in triplicate. The primers were designed for use in mice (*Mus musculus*) and described in Table 1.

Statistical analysis

Initially, all data were analyzed for normality. For the in vivo size injury and gene expression tests, the one-way analysis of variance (ANOVA) was applied, followed by post hoc Tukey. The statistical program used was SPSS (version 16.0—SPSS, Chicago, IL, USA) and the significance level used in the study was 5% ($p < 0.05$).

Results

The cells were seeded on the scaffolds for seven days and following this the construction was used in animal experiments with athymic mice. The analysis by confocal microscopy revealed the presence of MSCs on one side of the biomaterial and keratinocytes on the other side. MSCs can be recognized by their morphology, with elongated cytoplasm in both types of scaffolds tested (Figure 1(a) and (b)). The keratinocytes can

Table 1. *Primers* used in real-time PCR.

Primer	*Forward sequence*	*Reverse sequence*
GAPDH[34]	AGGTCGGTGTGAACGGATTTG	TGTAGACCATGTAGTTGAGGTCA
Col1a1[35]	GGTCTTGGTGGTTTTGTATTCG	AACAGTCGCTTCACCTACAGC
TGF-β1[26]	TATTTGGAGCCTGGACACAC	CTTGCGACCCACGTAGTAGA
SDF-1[26]	GTCTAAGCAGCGATGGGTTC	GAATAAGAAAGCACACGCTGC
VEGF[36]	TGTACCTCCACCATGCCAAGT	TGGAAGATGTCCACCAGGGT
BAX[37]	CACAGCGTGGTGGTACCTTA	TCTTCTGTACGGCGGTCTCT
Bcl-2[37]	TCGCAGAGATGTCCAGTCAG	ATGCCGGTTCAGGTACTCAG

GAPDH: glyceraldehyde 3-phosphate dehydrogenase.

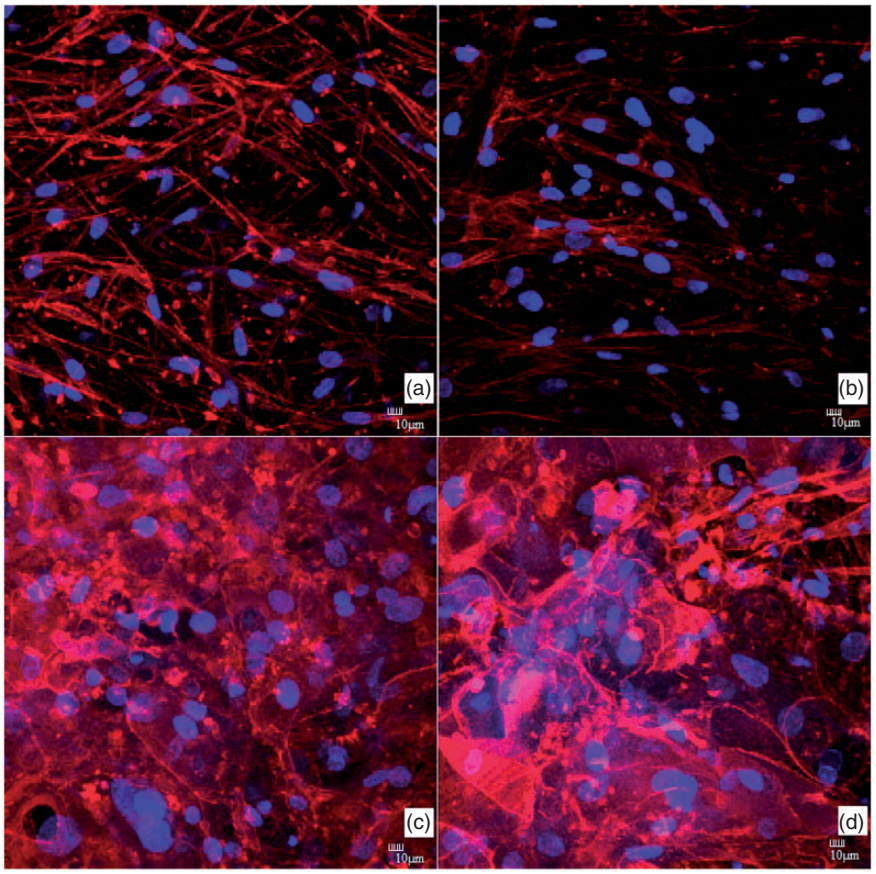

Figure 1. Confocal microscopy analysis of the MSCs and keratinocytes after seven days of sowing on the scaffolds. (a) MSCs on PDLLA matrix, (b) MSC on PDLLA/Lam matrix, (c) keratinocytes on PDLLA matrix, and (d) keratinocytes on PDLLA/Lam matrix.

also be recognized by their morphology in both biomaterials (Figure 1(c) and (d)). Thus, the scaffolds used in animal PDLLA + cells and PDLLA/Lam + cells groups showed both cell types at the time of implantation in the athymic mice.

Surgeries were performed in 28 animals. A further four animals were used as healthy controls. None of the animals showed signs of infection throughout the analysis period. There was also no animal loss.

To measure the average size of the lesions after nine days of surgery, five groups were tested: (1) lesion control, (2) PDLLA/Lam, (3) PDLLA, (4) PDLLA/Lam + cells, and (5) PDLLA + cells. Initially, all the animals received the same lesion standard, and after nine days the mean and standard deviations for groups 1, 2, 3, 4, and 5 were $0.319 \pm 0.040\,cm^2$, $0.315 \pm 0.056\,cm^2$, $0.439 \pm 0.117\,cm^2$, $0.342 \pm 0.110\,cm^2$, and $0.411 \pm 0.170\,cm^2$, respectively

(Figure 2). There was no statistical difference between the different groups ($p = 0.296$), although groups 2 and 4 (PDLLA/Lam scaffolds without and with cells, respectively) had a greater reduction in the injured area when compared to groups 3 and 5 (PDLLA scaffolds without and with cells).

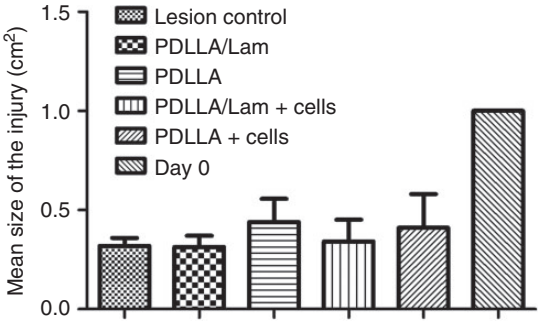

Figure 2. Graph of mean size of the lesion after nine days of surgery with total removal of skin. Day 0 corresponds to the size of the injury immediately after the excision of the skin.

In the groups where the MSCs and keratinocytes were previously seeded on the matrices (groups 4 and 5), it was still possible to visualize the entire scaffolds on the injury after nine days of surgery. In three out of six animals from group 3, it was also possible to view some parts of the scaffolds (Figure 3).

Regarding the visual aspect of the wound bed, group 2 (PDLLA/Lam) presented the greatest visual aspect, without the formation of a coarse wound. However, group 1, lesion control, showed the worst aspect in the injury bed (Figure 4). Furthermore, the area removed for analysis only comprised the wound site, thus, the second group appeared to present the smallest wound contraction because, after removal of the damaged area, it was the group with the smallest size injury, that is, there was no expansion of the injured area after removal of the scar tissue (Figure 4).

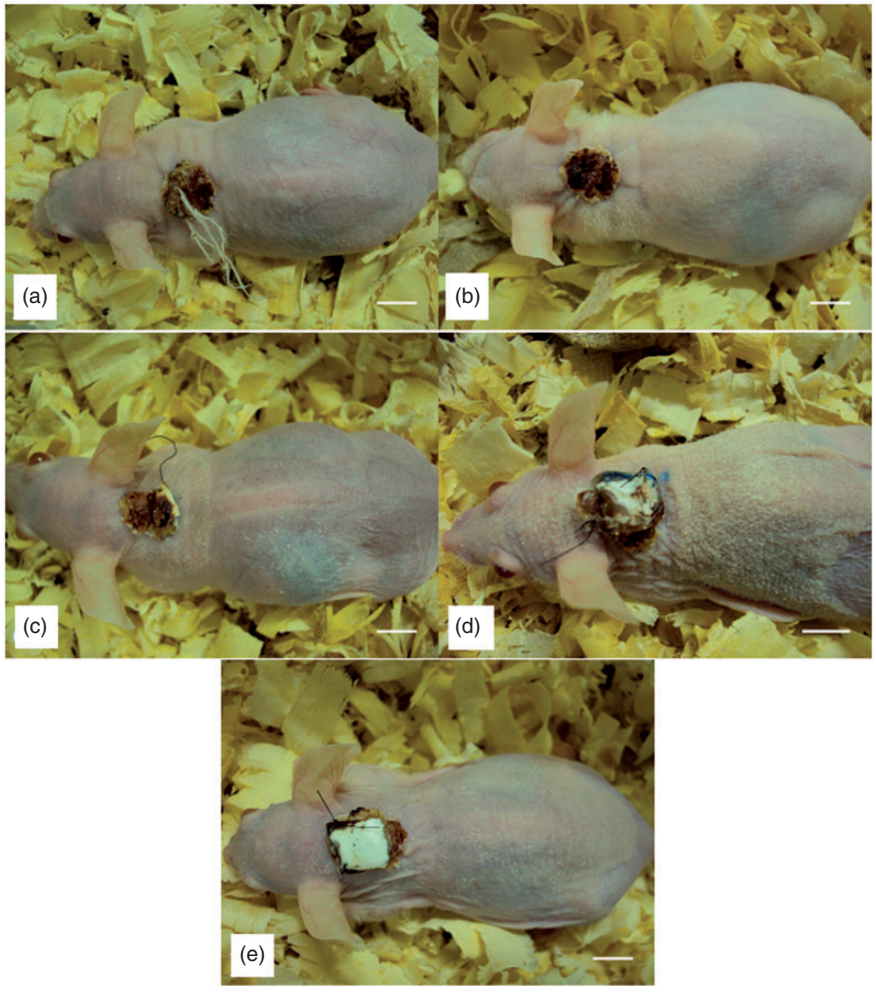

Figure 3. Photographs of the cutaneous lesions of the animals nine days after surgery. (a) Lesion control, (b) PDLLA/Lam, (c) PDLLA, (d) PDLLA/Lam + cells, and (e) PDLLA + cells. The scale bar corresponds to 1 cm.

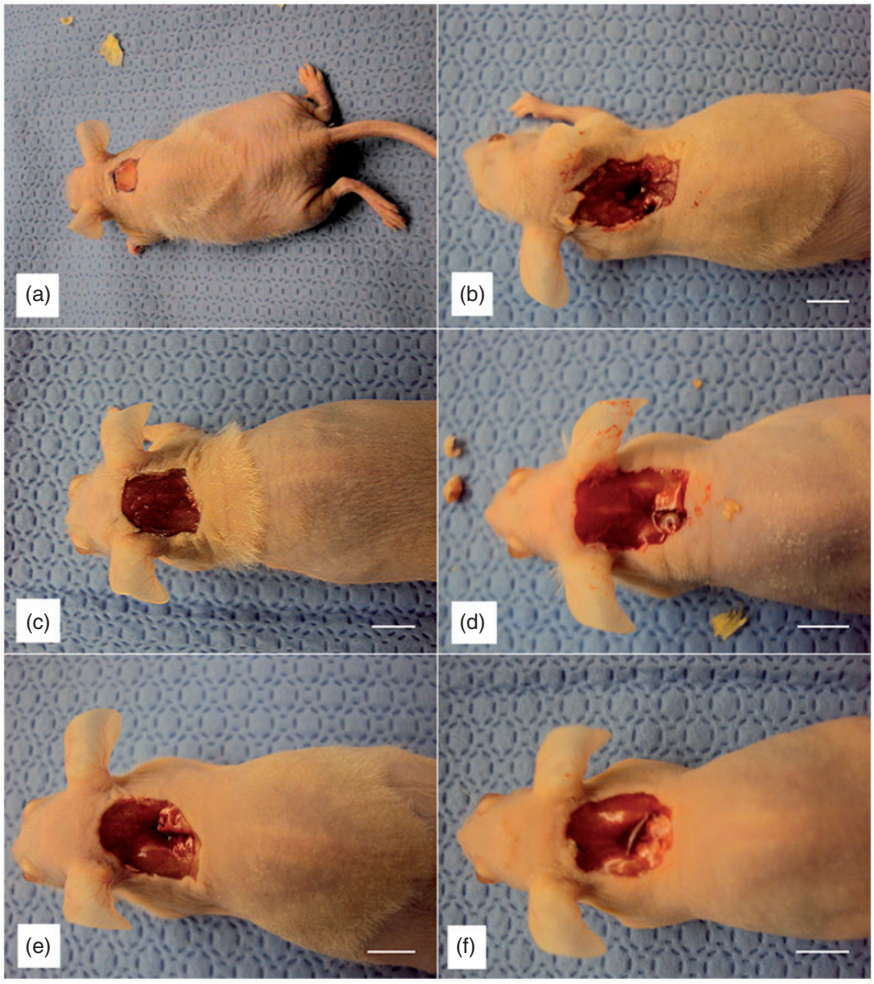

Figure 4. Photographs of the skin lesion bed on the day of surgery (a) and post nine days surgery. (b) Lesion control, (c) PDLLA/Lam, (d) PDLLA, (e) PDLLA/Lam + cells, and (f) PDLLA + cells. The scale bar corresponds to 1 cm.

Gene expression was performed comparing the evaluated genes between the tested groups (Figure 5).

Regarding the Bcl-2 gene, the PDLLA, PDLLA + cells, and healthy control groups showed an increase in gene expression compared to the lesion control group, with statistically significant difference ($p = 0.012$, $p < 0.001$, and $p = 0.041$, respectively). The others groups did not differ, although the PDLLA/Lam group presented a trend toward statistical difference ($p = 0.072$).

All the groups showed an upregulation of vascular endothelial growth factor (VEGF) when compared to the lesion control group. The fourth group (PDLLA/Lam + cells) showed the highest gene expression of VEGF, which was statistically different from group 1 (control lesion; $p < 0.001$), 3 (PDLLA; $p = 0.039$), 5 (PDLLA + cells; $p = 0.003$), and 6 (healthy control; $p = 0.011$), and similar to group 2 (PDLLA/Lam; $p = 0.1$).

In the gene expression of TGFβ1, all the groups that had implanted biomaterials were statistically different from the control group ($p < 0.014$ for all comparisons) and expressed considerably more TGFβ1.

For the gene of type I pro-collagen, only group 6 (healthy control) was different to the lesion control group ($p = 0.007$). Groups 2 and 5 showed no statistical difference when compared to group 6 in terms of gene expression ($p = 0.056$ and $p = 0.822$, respectively).

In the SDF-1 expression, group 3 showed the highest expression, presenting statistical difference with the lesion control group and the other groups ($p < 0.001$ in all cases).

There was no statistical difference between all the groups tested and the healthy control in terms of gene expression of BAX. When comparing the groups where biomaterials were implanted in the lesion control group, the difference only occurred between groups 4 and 5

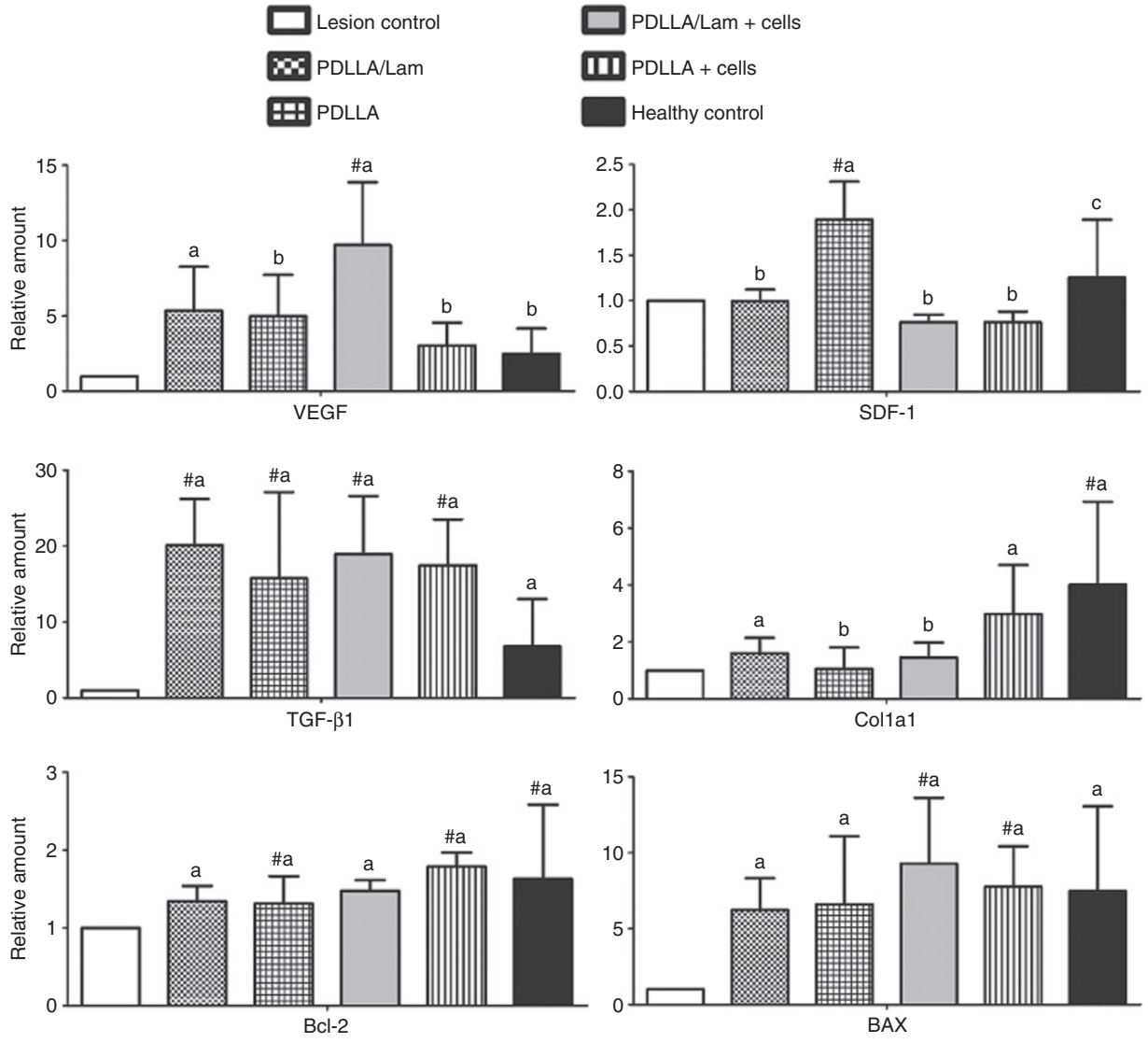

Figure 5. Gene expression of the different groups tested for Bcl-2, VEGF, TGFβ1, Col1a1, SDF-1, and BAX genes. # Refers to the comparison to the lesion control group. The letters refer to the comparisons made between the other groups for the same gene in question. GAPDH was used as a housekeeping gene and all the data were normalized against the housekeeping gene.

($p = 0.001$ and $p = 0.015$, respectively). The control group had the lowest injury levels of BAX expression.

Histological analysis was performed in the same groups analyzed for gene expression and photomicrographs can be seen in Figure 6. The skin appendages, such as sebaceous glands and hair follicles, were not observed in any of the animals tested, except for the healthy animals (Figure 6(o) and (p)).

Through Figure 6(a), it is possible to see that the control group showed a more disorganized injury in the lesion area after nine days. The dermis presented blood vessels, as well as a large inflammatory infiltrate (Figure 6(b)). Although blood vessels are observed in the images relating to the animals of the lesion control group, the groups in which the biomaterials were used visually present an increased vascularization, with the distribution of red blood cells throughout the tissue.

In the PDLLA/Lam (Figure 6(c) to (e)) and PDLLA (Figure 6(f) to (h)) groups, a similarity in the histological organization is observed, with well-formed and arranged dermis, both near the edges of the lesion and the central region. The epidermis in these two groups is well-formed near the edges, but not in the central region, where it was still possible to verify the presence of granulation tissue with inflammatory infiltrate (Figure 6(e) and (g)). In Figure 6(e), the place the inflammatory cells was occupying is similar to the scaffold structure, already in an advanced state of degradation. In Figure 6(h) it is still possible to view the whole PDLLA scaffold above the injury.

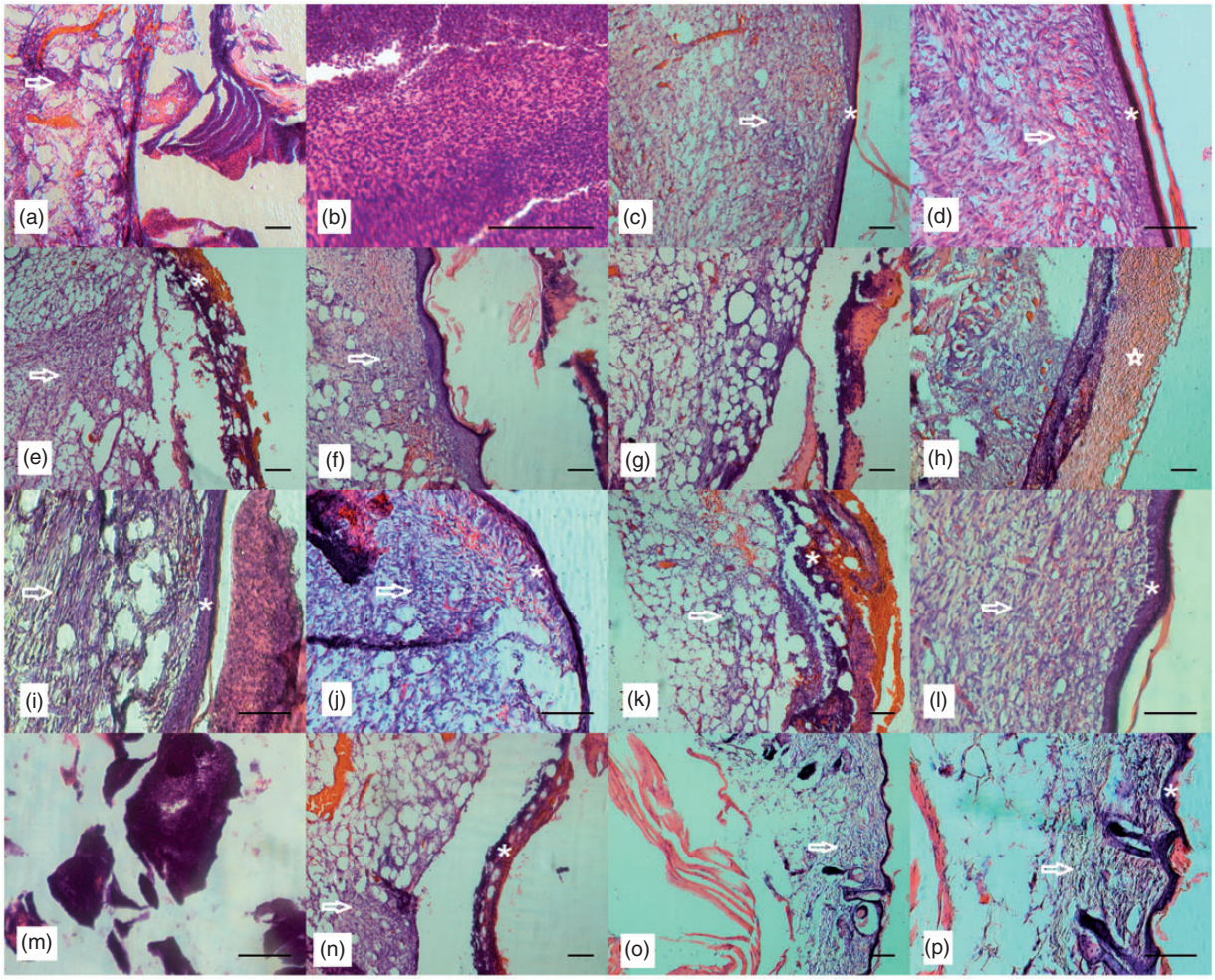

Figure 6. Photomicrographs of histological analysis of tissue related to the in vivo experiments. The samples were stained with hematoxylin–eosin stains. (a) and (b) refer to the lesion control group. (a) Appearance of injury nine days after the experiment, with the disorganized dermis and absence of epidermis; (b) inflammatory infiltrate present in the wound bed. (c–e) Correspond to the PDLLA/Lam group. (c) Well-formed dermis and epidermis next to the edge of the lesion; (d) magnification of the same region of partfigure (c), where the epidermis is most prominent with the presence of stratum corneum; (e) central region of the lesion with partially formed dermis and the formation of the epidermis with the presence of granulation tissue. (f)–(h) Refer to the PDLLA group. (f) Region next to the edge of the lesion in which can be viewed well-formed dermis and epidermis; (g) central region with prominent granulation tissue and presence of inflammatory cells; (h) view of non-degraded scaffold on the skin lesion. (i)–(k) Correspond to the PDLLA/Lam + cells group. (i) Portion of the central region of the lesion displaying well-formed epidermis and dermis, with some granulation tissue and presence of inflammatory infiltrate; (j) central region where the formation of the epidermis is observable and with complete dermis; (k) central region of the lesion where the dermis and especially epidermis are in formation. (l)–(n) Refer to the PDLLA + cells group. (l) Image obtained from the central region of the lesion, with the dermis and the epidermis well formed; (m) presence of large inflammatory infiltrate in the region adjacent to the lesion; (n) formed dermis and epidermis in formation in the central region of the injury. (o) and (p) Correspond to the healthy control group. (o) Aspect of healthy skin, with the presence of the epidermis, dermis, and its annexes, as well as muscle tissue; (p) greater detail in the photomicrograph, where the hair follicles, the sebaceous glands, the epidermis with the stratum corneum, dermis, and below, the muscle tissue are displayed. The asterisk corresponds to the epidermis. The dermis is highlighted by the arrow. The star shows the scaffold. Scale bar: 20 μm.

In the groups where the MSCs and keratinocytes were seeded onto the scaffolds prior to implantation in the injury, it was possible to visualize the formation of the epidermis in the central region of the wound in two animals of each group (Figure 6(i) and (l), respectively for PDLLA/Lam + cells and PDLLA + cells groups). In the other animals from these groups, the central part of the injury resembles that found in the groups where the biomaterials were implanted without the cells (group PDLLA/Lam and PDLLA), as can be seen in Figure 6(k) and (n). Furthermore, one animal of the PDLLA/Lam group also showed the initial

formation of the epidermis in the central area, as displayed in Figure 6(j). A large inflammatory infiltrate was observed in the PDLLA + cell group (Figure 6(f)).

Discussion

The skin is the body's largest organ of vertebrates, being composed of epidermis and dermis. In this work, a bilayer biomaterial was produced for use as a skin substitute with the aim of mimicking conventional histology of the entire skin. The development of a biomaterial with different fiber morphologies at the top and bottom was possible and has already been characterized in a previous study.[22] The purpose of the construction of both fibers was to set different topologies to mimic the epidermis and dermis, or a bilayer generated by tissue engineering. Moreover, the linkage of a protein naturally encountered in skin, the laminin-332, was performed. Following this, keratinocytes were cocultured with MSCs in a nano- and micro-structured scaffold from a PDLLA polymer, mimicking the epidermis and dermis, respectively. In this work, it was demonstrated that the biomaterials behave well, being noncytotoxic, and provided a good environment for growth of the MSCs and keratinocytes. Moreover, it was also shown that these cells occupied all the structure of the scaffolds in a tridimensional architecture.[22]

The use of cells in tissue engineering is part of the triad for the development of materials. Thus, the MSCs were selected as the cellular component of the dermal substitute because of their ability to differentiate. The immunomodulatory capability of these cells has been reported in several studies,[28–30] which may be an advantage for their use, especially in severe conditions, such as with burn patients, although recently this property has been questioned.[31–33] Keratinocytes were the most predominant cells in the epidermis and they are responsible for the impermeability of the skin.

As the results for physicochemical and biological analysis were satisfactory for the biomaterials,[22] the next stage was to evaluate them in a skin loss animal model. Athymic mice were used because they lack mature T lymphocytes and thus they are not able to develop transplant rejection in other species,[34] as human cells used in this study.

The choice for using scaffolds with cells seven days after immersed cultivation for implantation in animals was taken in relation to results obtained in the previous study that showed that in this period it is possible to view the MSCs at the bottom and keratinocytes at the top of the matrices. After this time, the differentiation between the cells was no longer possible as they occupied all the structure.

The time of the in vivo experiments was based on the daily monitoring of the animals. Nine days after surgery, only the scaffolds where the cells had been seeded still showed themselves to be intact with no signs of degradation.

Regarding the size of the lesion after nine days, there was no statistical difference between the five groups tested; however, the groups of PDLLA/Lam, with or without cells, showed the most visual reduction of lesion size. These scaffolds without cells also showed the best appearance of the wound bed after the withdrawal of the newly formed tissue. The visual size analysis of all the animals after the withdrawal of the new tissue showed that the PDLLA/Lam group had the most attractive appearance of the injury, with no bloody area. Moreover, after the removal of the surroundings of the newly formed tissue, this group showed the lowest expansion of the lesion size compared with the lesion size where the skin was not removed in the regeneration process.

In order to verify the skin regeneration process in terms of gene expression, several genes were evaluated. Among these, the VEGF and stromal cell-derived factor 1 (SDF-1) related to vasculogenesis; TGFβ1 and type I procollagen (Col1a1), as fibrotic genes; and the genes of the Bcl family, such as Bcl-2, an antiapoptotic gene, and BAX, a proapoptotic gene were analyzed in the animal tissue.

During the process of formation and/or regeneration of tissue, angiogenesis is a critical process. It ensures the delivery of the required nutrients and oxygen at the lesion site, thus allowing for the formation of the granulation tissue. Two growth factors are therefore mutually related. VEGF is known to be the most responsible gene for angiogenesis. It is known that this factor is increased in the acute phase of the injury and its expression is induced within 24 h after skin injury, with a maximum peak at two to three days, declining to baseline levels after seven days.[35–37] In experiments conducted by Fronza et al.,[38] increased presence of VEGF after two days in rats with skin lesion was found, followed by decline thereafter. These animals were also accompanied for 21 days and increased vascularity was observed only seven days after performing the injury in the animals, i.e., after the elevation of VEGF.[38]

Another growth factor that has been drawing attention in recent years for its potential angiogenic capacity is the SDF-1. It has some similarities to VEGF, such as its chemotactic properties, its action on hematopoietic stem cells, endothelial progenitor cells, and mature endothelial cells[39,40] and the fact that it can also be produced by tumors and injured organs. Furthermore, both factors can regulate each other, increasing their expressions.[40]

Regarding the expression of these genes, VEGF showed the largest upregulation. When comparing the

different groups, the animals where biomaterials were implanted had higher VEGF expression when compared to the healthy control group, which was an expected result because the injured animals are in intense angiogenic process and thus a higher level of VEGF is required. In this context, the biomaterials appear to have had an advantage over the lesion control group, as more angiogenic activity was taking place, the healing became easier and aesthetically better. Previous studies show that low rates of oxygen due to microcirculatory abnormalities present in skin lesions induce increased TGFβ1 gene expression, a gene that when overexpressed can lead to the formation of hypertrophic scars and keloids.[41] On the other hand, the level of SDF-1 did not change much between the different groups, although there was statistical difference between the lesion control group and PDLLA group, with the greatest expression in the latter group. The previous presence of cells in the biomaterials does not seem to have affected the stimulation of expression of the vasculogenic genes.

Type I collagen synthesis is highly regulated by different cytokines at the transcriptional level. Especially TGFβ1 and TGFβ2, isoforms members of TGF family, which increases the expression of type I collagen gene and have a determining effect on wound healing and fibrosis.[42] Regarding the TGF, there was a substantial increase in all the tested groups compared to the lesion and healthy control groups. Compared with the healthy control group, this response was expected because the damage to the animals caused fibrotic effects in an attempt to close the caused injury, which did not occur to the healthy control animals. The increase of TGFβ1 in the animals in which the biomaterial was implanted was statistically different compared to the lesion control group. One possibility is the higher organization of the cells in these animals as the matrices could be acting as a bridge where cells are anchored and, thus, the beginning of the synthesis of collagen and consequent healing is faster. The initial presence of cells in the biomaterials does not seem to have affected, either positively or negatively, the stimulation of TGFβ1 gene expression.

Also in terms of wound healing, collagen is a major component of connective tissue. Thus, the healing process depends on its regulation, production, deposition, and subsequent maturation. The correct balance between synthesis and catabolism is important to prevent the formation of hypertrophic scars and keloids.[43] Moreover, in the initial stage of regeneration of skin lesions, collagen synthesis and deposition are essential, as Lu et al. demonstrated, using an anti-TGFβ at this stage, delaying the healing process.[44] On gene expression, Col1a1 only presented statistical difference in the healthy and lesion control groups. This absence of substantial increase in the tested groups may have been caused by the early timing of analysis. It is known that following injury, the TGFβ1 has an increase in its expression, which results in increased expression of the Col3a1 and Col1a1 genes, in sequence, respectively.[45] Thus, type I collagen is a later collagen to appear and it may have been the explanation for not having a substantial increase. Witte and Barbul demonstrated in their review on dermal regeneration progression that the deposition of type III collagen occurs hours after injury, whereas the type I collagen only starts to be deposited on the second day of injury. However, from the third-day post-injury, the synthesis of collagen type I already exceeds the type III collagen.[46] Regardless of this the PDLLA/Lam and PDLLA + cells groups presented statistically similar gene expression in comparison with the healthy control group, showing a healthy level of expression of this gene, although it was expected that all the groups would present a greater need for producing collagen fibers, and therefore upregulation of this gene.

Due to the use of different materials and different cells in the animal model, it generated an inquiry if these biomaterials could not influence the cellular activity of the animal cells, stimulating apoptosis, for example. Thus, the Bcl gene family was investigated. Intracellularly, induction of apoptosis is partly mediated by several genes, such as p53, Bcl-2, Bax, and p21. It is known that increasing the expression of Bcl-2 inhibits apoptosis induced by a variety of stimuli, whereas BAX predominance on Bcl-2 accelerates apoptosis upon apoptotic stimuli.[45] Furthermore, the BAX/Bcl-2 ratio determines the susceptibility of cells to apoptosis, i.e., the greater the amount of BAX and/or the smaller the amount of Bcl-2, the more susceptible the cell will be to apoptosis.[41] As can be seen in Figure 5, with respect to the expression of both genes, there was no statistical difference between the groups with biomaterials and the healthy control group. The BAX/Bcl-2 ratio also became quite similar, which can be observed by the similarity in the expression level between these genes in the groups with the biomaterials and the healthy control group. Moreover, the groups in which the cells were seeded on the scaffolds also showed no difference, indicating that they are not harmful in terms of cellular apoptosis. On the other hand, the lesion control group had much lower expression of both genes in comparison with all the other groups, although there was no statistical difference for all the comparisons.

Histological analysis of the different groups corroborated some results of gene expression analysis, as will be discussed below.

The lesion control group had the lowest levels of VEGF and Col1a1 expression and the largest

BAX/Bcl-2 imbalance, as well as showed the most disorganized tissue, with no observation of the formation of epidermis in any animal, contrary to what occurred in all the other groups. The lower vascularization probably favored the formation of a more aesthetically coarse wound. Furthermore, the great inflammatory infiltrate still present after nine days in the wound bed showed that this tissue was still in early stages of tissue regeneration.[38]

Although the formation of an epidermal layer near the edges of the skin defect in the PDLLA and PDLLA/Lam groups and also in the central region in the PDLLA/Lam + cells and PDLLA + cells groups in all the animals with biomaterials and biomaterials with cells was evident, the presence of skin attachments was not visualized, as in the healthy skin, indicating that, although there was skin regeneration, this was not structurally complete. In a separate work, Dearman and Lorden also demonstrated tissue regeneration with biomaterials with newly formed vascularized tissue in 7–10 days after the skin lesion, without the formation of skin attachments.[47,48] Dearman also observed in histological analysis in pigs after 21 days of experimentation a complete formation of the epidermis and on this the presence of a carapace composed of the implanted biomaterial along with keratinocytes and fibroblasts.[47] In the present study, the same was observed in the athymic mice in which were applied biomaterials + cells. As can be seen in Figures 3 and 6, in some animals, all the biomaterials were present on the injury, but in some of them, it was possible to view the epidermis in the full extent of the wound.

The cells seeded on the biomaterials, in this context, appeared to have had a beneficial effect on wound healing because they stimulated the production of a complete epidermal layer in some of the animals, as can be observed in the PDLLA/Lam + cells and PDLLA + cells groups. This fact offers an advantage in relation to their use in burn patients because they might thereby be less exposed to the external environment and hence less susceptible to infections.

In terms of regeneration of the dermal layer, there was no difference between the different animals treated with biomaterials and biomaterials + cells as they all had well-formed dermis. This ultimately demonstrates the ability of the scaffold to act as a bridge, where the cells from the receptor may anchor to produce new tissue considering that even biomaterials in which the cells were not previously seeded were capable of producing histologically homogeneous tissue.

In some biomaterials, it was also possible to verify the presence of inflammatory cells, especially in places where regeneration was still occurring. This phenomenon took place less in the groups with biomaterials compared to that found in the lesion control group, which demonstrates that granulation tissue was being generated or had already been generated, and the formation of the new tissue was the next step to occur. In a paper developed by Lorden et al., using wild-type mice, it was also possible to verify the presence of moderate inflammatory infiltrate after 30 days of the skin lesion, as a part of the acute inflammatory response to guide skin regeneration.[48] Thus, mild inflammation appears to be required for the correct regeneration process as opposed to the injury which occurred in the lesion group, where the more pronounced inflammation seemed to cause a heterogeneous healing, forming a disorganized tissue.

Hence, by the results obtained in the gene expression and histological analysis, it was not possible to determine a possible advantage in the use of laminin protein in PDLLA/Lam biomaterials compared to PDLLA biomaterials, although through visual analysis and wound size, this protein has shown noticeable advantages.

Conclusion

Due to the results obtained in this study, the intention is to conduct further animal experiments and track the same analysis for a longer period of time, checking the wound closure in all the animals for gene expression tests and histological analysis to then be carried out; the aim of this being to have a real view of the effects of laminin on the healing of the animals. However, with the results presented here, it was verified that the produced biomaterials were effective in tissue healing and showed real advantages compared to the lesion control group, which presents them as potential biomaterials for use in skin tissue engineering.

Declaration of Conflicting Interests

The author(s) declared no potential conflicts of interest with respect to the research, authorship, and/or publication of this article.

Funding

The author(s) disclosed receipt of the following financial support for the research, authorship, and/or publication of this article: This work was supported by CNPq, CAPES, FAPERGS and the Stem Cell Research Institute.

References

1. Harris MINC. *Pele: estrutura, propriedades e envelhecimento*. Terceira edição ed. São Paulo: Senac, 2009.
2. Peyrefitte G, Martini MC and Chivot M. *Cosmetologia, biologia geral e biologia da pele*. Terceira edição ed. São Paulo: Andrei, 1998.

3. Mohd Hilmi AB and Halim AS. Vital roles of stem cells and biomaterials in skin tissue engineering. *World J Stem Cells* 2015; 7: 428–436.
4. Gamonal A. *Dermatologia elementar: compêndio de dermatologia*. Segunda edição ed. Juiz de Fora: Sampaio & Rivitti, 2002.
5. Supp DM and Boyce ST. Engineered skin substitutes: practices and potentials. *Clin Dermatol* 2005; 23: 403–412.
6. Burd A, Ayyappan T and Huang L. Cord blood: opportunities and challenges for the reconstructive surgeon. In: Bhattacharya N and Stubblefield P (eds) *Frontiers of cord blood science*, 1st ed. London: Springer, 2009, pp. 273–287.
7. Leite F. Apagão traz risco de queimaduras. Folha Online, 2001.
8. Sun BK, Siprashvili Z and Khavari PA. Advances in skin grafting and treatment of cutaneous wounds. *Science* 2014; 346: 941–945.
9. Venugopal JR, Prabhakaran MP, Mukherjee S, et al. Biomaterial strategies for alleviation of myocardial infarction. *J R Soc Interface* 2012; 9: 1–19.
10. Metcalfe AD and Ferguson MW. Tissue engineering of replacement skin: the crossroads of biomaterials, wound healing, embryonic development, stem cells and regeneration. *J R Soc Interface* 2007; 4: 413–437.
11. Wang C, Chien HS and Yan KW. Correlation between processing parameters and microstructure of electrospun poly(D,L-lactic acid) nanofibers. *Polymer* 2009; 50: 6100–6110.
12. Blaker JJ, Gough JE, Maquet V, et al. In vitro evaluation of novel bioactive composites based on Bioglass-filled polylactide foams for bone tissue engineering scaffolds. *J Biomed Mater Res A* 2003; 67: 1401–1411.
13. Roether JA, Boccaccini AR, Hench LL, et al. Development and in vitro characterisation of novel bioresorbable and bioactive composite materials based on polylactide foams and bioglass for tissue engineering applications. *Biomaterials* 2002; 23: 3871–3878.
14. Maquet V, Boccaccini AR, Pravata L, et al. Porous poly(alpha-hydroxyacid)/bioglass composite scaffolds for bone tissue engineering. I: preparation and in vitro characterisation. *Biomaterials* 2004; 25: 4185–4194.
15. Steffens D, Lersch M, Rosa A, et al. A new biomaterial of nanofibers with the microalga Spirulina as scaffolds to cultivate with stem cells for use in tissue engineering. *J Biomed Nanotechnol* 2013; 9: 710–718.
16. Chiang LY, Poole K, Oliveira BE, et al. Laminin-332 coordinates mechanotransduction and growth cone bifurcation in sensory neurons. *Nat Neurosci* 2011; 14: 993–1000.
17. Sugawara K, Tsuruta D, Ishii M, et al. Laminin-332 and -511 in skin. *Exp Dermatol* 2008; 17: 473–480.
18. Domogatskaya A, Rodin S and Tryggvason K. Functional diversity of laminins. *Ann Rev Cell Dev Biol* 2012; 28: 523–553.
19. Boccafoschi F, Fusaro L, Mosca C, et al. The biological response of poly(L-lactide) films modified by different biomolecules: role of the coating strategy. *J Biomed Mater Res A* 2012; 100: 2373–2381.
20. Mammadov B, Mammadov R, Guler MO, et al. Cooperative effect of heparan sulfate and laminin mimetic peptide nanofibers on the promotion of neurite outgrowth. *Acta Biomater* 2012; 8: 2077–2086.
21. Hozumi K, Sasaki A, Yamada Y, et al. Reconstitution of laminin-111 biological activity using multiple peptide coupled to chitosan scaffolds. *Biomaterials* 2012; 33: 4241–4250.
22. Steffens D, Mathor MB, Santi BTs, et al. Development of a biomaterial associated with mesenchymal stem cells and keratinocytes for use as a skin substitute. *Regen Med* 2015; 10: 975–987.
23. Herson MR, Mathor MB, Altran S, et al. In vitro construction of a potential skin substitute through direct human keratinocyte plating onto decellularized glycerol-preserved allodermis. *Artif Organs* 2001; 25: 901–906.
24. Tanikawa DY, Alonso N, Herson MR, et al. Ultrastructural evaluation of human keratinocyte growth and differentiation on a fibrin substrate. *Acta Cir Bras* 2010; 25: 541–548.
25. Leonardi D, Oberdoerfer D, Fernandes MC, et al. Mesenchymal stem cells combined with an artificial dermal substitute improve repair in full-thickness skin wounds. *Burns* 2012; 38: 1143–1150.
26. Powell HM, Supp DM and Boyce ST. Influence of electrospun collagen on wound contraction of engineered skin substitutes. *Biomaterials* 2008; 29: 834–843.
27. Akinbingol G, Borman H, Maral T, et al. Wound healing at adaptation zones of skin flaps harvested from acute burned skin. *Burns* 2013; 39: 1206–1211.
28. Caplan AI. Adult mesenchymal stem cells for tissue engineering versus regenerative medicine. *J Cell Physiol* 2007; 213: 341–347.
29. Silva FeS, Ramos RN, de Almeida DC, et al. Mesenchymal stem cells derived from human exfoliated deciduous teeth (SHEDs) induce immune modulatory profile in monocyte-derived dendritic cells. *PLoS One* 2014; 9: e98050.
30. Remacha AR, Barrachina L, Álvarez-Arguedas S, et al. Expression of genes involved in immune response and in vitro immunosuppressive effect of equine MSCs. *Vet Immunol Immunopathol* 2015; 165: 107–118.
31. Kronsteiner B, Wolbank S, Peterbauer A, et al. Human mesenchymal stem cells from adipose tissue and amnion influence T-cells depending on stimulation method and presence of other immune cells. *Stem Cells Dev* 2011; 20: 2115–2126.
32. Sánchez-Abarca LI, Alvarez-Laderas I, Díez Campelo M, et al. Uptake and delivery of antigens by mesenchymal stromal cells. *Cytotherapy* 2013; 15: 673–678.
33. Ankrum JA, Ong JF and Karp JM. Mesenchymal stem cells: immune evasive, not immune privileged. *Nat Biotechnol* 2014; 32: 252–260.
34. Andrade, A, Pinto, SC and Oliveira RS., Orgs. *Animais De Laboratório: Criação E Experimentação* [Online]. Rio De Janeiro: Editora Fiocruz, 2002, p. 388. ISBN: 85-7541-015-6. Available From Scielo Books.
35. Brown LF, Yeo KT, Berse B, et al. Expression of vascular permeability factor (vascular endothelial growth

factor) by epidermal keratinocytes during wound healing. *J Exp Med* 1992; 176: 1375–1379.
36. Shukla A, Dubey MP, Srivastava R, et al. Differential expression of proteins during healing of cutaneous wounds in experimental normal and chronic models. *Biochem Biophys Res Commun* 1998; 244: 434–439.
37. Martino MM, Brkic S, Bovo E, et al. Extracellular matrix and growth factor engineering for controlled angiogenesis in regenerative medicine. *Front Bioeng Biotechnol* 2015; 3: 45.
38. Fronza M, Caetano GF, Leite MN, et al. Hyaluronidase modulates inflammatory response and accelerates the cutaneous wound healing. *PLoS One* 2014; 9: e112297.
39. Mirshahi F, Pourtau J, Li H, et al. SDF-1 activity on microvascular endothelial cells: consequences on angiogenesis in in vitro and in vivo models. *Thromb Res* 2000; 99: 587–594.
40. Petit I, Jin D and Rafii S. The SDF-1-CXCR4 signaling pathway: a molecular hub modulating neo-angiogenesis. *Trends Immunol* 2007; 28: 299–307.
41. Sultan SM, Barr JS, Butala P, et al. Fat grafting accelerates revascularisation and decreases fibrosis following thermal injury. *J Plast Reconstr Aesthet Surg* 2012; 65: 219–227.
42. Walraven M, Beelen RH and Ulrich MM. Transforming growth factor-β (TGF-β) signaling in healthy human fetal skin: a descriptive study. *J Dermatol Sci* 2015; 78: 117–124.
43. Santibañez JF, Quintanilla M and Bernabeu C. TGF-β/TGF-β receptor system and its role in physiological and pathological conditions. *Clin Sci (Lond)* 2011; 121: 233–251.
44. Lu L, Saulis A, Liu W, et al. The temporal effects of anti-TGF-beta 1, 2, and 3 monoclonal antibody on wound healing and hypertrophic scar formation. *J Am Coll Surg* 2005; 201: 391–397.
45. Jurzak M, Adamczyk K, Antończak P, et al. Evaluation of genistein ability to modulate CTGF mRNA/protein expression, genes expression of TGFβ isoforms and expression of selected genes regulating cell cycle in keloid fibroblasts in vitro. *Acta Pol Pharm* 2014; 71: 972–986.
46. Witte MB and Barbul A. General principles of wound healing. *Surg Clin North Am* 1997; 77: 509–528.
47. Dearman BL, Li A and Greenwood JE. Optimization of a polyurethane dermal matrix and experience with a polymer-based cultured composite skin. *J Burn Care Res* 2014; 35: 437–448.
48. Lorden ER, Miller KJ, Bashirov L, et al. Mitigation of hypertrophic scar contraction via an elastomeric biodegradable scaffold. *Biomaterials* 2015; 43: 61–70.